

RESEARCH ARTICLE

# Apamin Boosting of Synaptic Potentials in $Ca_v2.3$ R-Type $Ca^{2+}$ Channel Null Mice

Kang Wang<sup>1</sup>, Melissa H. Kelley<sup>1</sup>, Wendy W. Wu<sup>2a</sup>, John P. Adelman<sup>1</sup>, James Maylie<sup>2\*</sup>

**1** Vollum Institute, Oregon Health & Science University, Portland, Oregon 97239, United States of America, **2** Department of Obstetrics and Gynecology, Oregon Health & Science University, Portland, Oregon 97239, United States of America

✉ Current address: FDA, White Oak Campus, Silver Spring, MD 20993, United States of America  
\* [mayliej@ohsu.edu](mailto:mayliej@ohsu.edu)

## Abstract

SK2- and  $K_v4.2$ -containing  $K^+$  channels modulate evoked synaptic potentials in CA1 pyramidal neurons. Each is coupled to a distinct  $Ca^{2+}$  source that provides  $Ca^{2+}$ -dependent feedback regulation to limit AMPA receptor (AMPA)- and NMDA receptor (NMDAR)-mediated postsynaptic depolarization. SK2-containing channels are activated by  $Ca^{2+}$  entry through NMDARs, whereas  $K_v4.2$ -containing channel availability is increased by  $Ca^{2+}$  entry through SNX-482 (SNX) sensitive  $Ca_v2.3$  R-type  $Ca^{2+}$  channels. Recent studies have challenged the functional coupling between NMDARs and SK2-containing channels, suggesting that synaptic SK2-containing channels are instead activated by  $Ca^{2+}$  entry through R-type  $Ca^{2+}$  channels. Furthermore, SNX has been implicated to have off target effects, which would challenge the proposed coupling between R-type  $Ca^{2+}$  channels and  $K_v4.2$ -containing  $K^+$  channels. To reconcile these conflicting results, we evaluated the effect of SK channel blocker apamin and R-type  $Ca^{2+}$  channel blocker SNX on evoked excitatory postsynaptic potentials (EPSPs) in CA1 pyramidal neurons from  $Ca_v2.3$  null mice. The results show that in the absence of  $Ca_v2.3$  channels, apamin application still boosted EPSPs. The boosting effect of  $Ca_v2.3$  channel blockers on EPSPs observed in neurons from wild type mice was not observed in neurons from  $Ca_v2.3$  null mice. These data are consistent with a model in which SK2-containing channels are functionally coupled to NMDARs and  $K_v4.2$ -containing channels to  $Ca_v2.3$  channels to provide negative feedback regulation of EPSPs in the spines of CA1 pyramidal neurons.

## Introduction

On hippocampal CA1 pyramidal neurons, dendritic spines are specialized membrane compartments that protrude from the dendrites and house proteins that mediate and shape excitatory postsynaptic responses[1]. Even within the small spine volume (~0.05 fL)[2], synaptic proteins are organized into discrete, functional domains. The postsynaptic density (PSD) is an electron-dense structure that contains ionotropic glutamate receptors, AMPARs and NMDARs that mediate excitatory postsynaptic responses. SK2-containing channels are also localized in the



## OPEN ACCESS

**Citation:** Wang K, Kelley MH, Wu WW, Adelman JP, Maylie J (2015) Apamin Boosting of Synaptic Potentials in  $Ca_v2.3$  R-Type  $Ca^{2+}$  Channel Null Mice. PLoS ONE 10(9): e0139332. doi:10.1371/journal.pone.0139332

**Editor:** Vadim E. Degtyar, University of California, Berkeley, UNITED STATES

**Received:** May 26, 2015

**Accepted:** September 11, 2015

**Published:** September 29, 2015

**Copyright:** This is an open access article, free of all copyright, and may be freely reproduced, distributed, transmitted, modified, built upon, or otherwise used by anyone for any lawful purpose. The work is made available under the [Creative Commons CC0](https://creativecommons.org/licenses/by/4.0/) public domain dedication.

**Data Availability Statement:** All relevant data are within the paper.

**Funding:** Funding provided by National Institute of Health, 5R01NS038880-15, JPA; National Institute of Health, 5R01MH093599-03, JPA.

**Competing Interests:** The authors have declared that no competing interests exist.

PSD[3]. These channels are activated by synaptically evoked  $Ca^{2+}$  influx through NMDARs, and their repolarizing conductance reduces glutamate-evoked excitatory postsynaptic responses and  $Ca^{2+}$  transients within the spine head. Thus, blocking synaptic SK2-containing channels with apamin increased EPSPs and the associated spine  $Ca^{2+}$  transients, while blocking NMDARs occludes the effects of apamin[4,5]. Several classes of ion channels and receptors reside in the extrasynaptic domain of the spine head. Among them are  $K_v4.2$ -containing  $K^+$  channels and  $Ca_v2.3$  R-type  $Ca^{2+}$  channels[6]. Previous experiments using glutamate uncaging onto individual spines or direct afferent stimulation have reached different conclusions about the role of R-type  $Ca^{2+}$  channels in regulating EPSPs in CA1 pyramidal neurons. While both sets of experiments showed that blocking R-type  $Ca^{2+}$  channels with SNX boosted EPSPs, the effects of SNX and apamin were mutually exclusive when spines were stimulated by glutamate uncaging, suggesting that SK2-containing channels are gated by  $Ca^{2+}$  influx through R-type  $Ca^{2+}$  channels[5]. In contrast, the boosting effects of SNX and apamin were additive when direct afferent stimulation was applied[7]. Subsequent work showed that the boosting effect of SNX on EPSPs induced by glutamate uncaging was lost in  $Ca_v2.3$  null mice[8]. However, a recent report showed that in addition to blocking R-type  $Ca^{2+}$  channels, SNX blocks A-type  $K^+$  currents in dissociated dopamine neurons from substantia nigra pars compacta and cloned  $K_v4.3$  channels were much more sensitive to SNX compared to  $K_v4.2$  channels[9]. Furthermore, in cerebellar stellate cells where T-type  $Ca^{2+}$  channels couple to A-type  $K^+$  currents SNX had no effect on A-type channel availability, nor in tsA-201 cells co-expressing R-type ( $Ca_v2.3$ ) channels with  $K_v4.2$ [10]. Therefore, we used synaptic stimulations to evoke EPSPs from CA1 pyramidal neurons in slices from  $Ca_v2.3$  R-type null mice to determine whether in the absence of  $Ca_v2.3$  channels, apamin and SNX still boosted EPSPs.

## Materials and Methods

### Animal Handling and Slice Preparation

All procedures were approved in accordance with the guidelines of the Institutional Animal Care and Use Committee (IACUC) of the Oregon Health & Science University (IACUC: IS00002421). Hippocampal slices were prepared from 4–6 week-old  $Ca_v2.3$  null ( $Ca_v2.3^{-/-}$ , C57BL/6J background) and wild type mice (C57BL/6J background). Mice were anesthetized by isoflurane, rapidly decapitated, and brains removed and placed into ice-cold sucrose-aCSF of the following composition (equilibrated with 95% $O_2$ /5% $CO_2$ ) [7]. Transverse hippocampal slices (300  $\mu$ m) were cut with a Leica VT1200S and transferred into a holding chamber containing regular aCSF (in mM: 125 NaCl, 2.5 KCl, 21.5  $NaHCO_3$ , 1.25  $NaH_2PO_4$ , 2.0  $CaCl_2$ , 1.0  $MgCl_2$ , 12 glucose) and equilibrated with 95% $O_2$ /5% $CO_2$ . Slices were incubated at 35°C for 30–45 min and then recovered at room temperature (22–24°C) for  $\geq 1$  hr before recordings were performed.

### Electrophysiology

CA1 pyramidal cells were visualized with infrared-differential interference contrast optics (Zeiss Axioskop 2FS, Zeiss Axio Examiner or Leica DM LFS). Whole-cell patch-clamp recordings were obtained from CA1 pyramidal cells using an Axopatch 1D (Molecular Devices, Sunnyvale, CA) interfaced to an ITC-16 analog-to-digital converter (Heka Instruments, Bellmore, NY), EPC 10 (Heka Instruments, Bellmore, NY) patch clamp amplifier or Multiclamp 700B interfaced to a Digidata 1440A (Molecular Devices, Sunnyvale, CA). Data were transferred to a computer using Patchmaster software (Heka Instruments, Bellmore, NY) or pClamp10 software (Molecular Devices, Sunnyvale, CA). Patch pipettes (open pipette resistance, 2.5–3.5  $M\Omega$ ) for EPSP recordings were filled with either a K-gluconate internal solution containing (in mM)

133 K-gluconate, 4 KCl, 4 NaCl, 2 MgCl<sub>2</sub>, 10 HEPES, 4 MgATP, 0.3 Na<sub>3</sub>GTP, 10 K-phosphocreatine (pH 7.3). EPSPs were recorded in whole-cell current-clamp mode and voltages were not corrected for a junction potential of -13 mV. All recordings used cells with a resting membrane potential less than -50 mV and a stable input resistance that did not change by more than 20%. Cells were biased to -65 mV and the input resistance was determined from a 25-pA hyperpolarizing current injection pulse given 500 ms after each synaptically evoked EPSP. There was not obvious difference in resting membrane properties in CA1 neurons from  $Ca_v2.3^{-/-}$  compared to WT (average input resistance =  $188.5 \pm 6.3$  M $\Omega$  (n = 55) in  $Ca_v2.3^{-/-}$  and  $201.4 \pm 8.6$  (n = 33) in WT; average bias current =  $-73.3 \pm 7.1$  pA (n = 55) in  $Ca_v2.3^{-/-}$  and  $-76.5 \pm 7.5$  pA (n = 33) for WT).

## Synaptic stimulation

CA3 axons in the stratum radiatum were stimulated using capillary glass pipettes filled with aCSF, with a tip diameter of  $\sim 5$   $\mu$ m, connected to an Iso-Flex (A.M.P.I., Israel) or Digitimer DS3 (Automate Scientific, Berkeley, Ca) stimulus isolation unit. Stimulation electrodes were placed at  $\sim 100$   $\mu$ m from the soma and  $\sim 20$   $\mu$ m adjacent to the dendrite of the recorded cell. GABAergic blockers SR95531 (2  $\mu$ M) and CGP55845 (1  $\mu$ M) were present throughout the recordings to block GABA<sub>A</sub> and GABA<sub>B</sub> receptors, respectively. To prevent recurrent excitation in the CA3 region in the presence of GABAergic blockers, the CA3 region was cut away before recording. Subthreshold EPSPs were elicited by 100- $\mu$ s current injections (20–30  $\mu$ A) that were approximately one-third of the stimulus required for evoking an action potential. No obvious difference in stimulation amplitude was observed between slices from  $Ca_v2.3^{-/-}$  and WT.

## Data analysis

Data were analyzed using Igor Pro (WaveMetrics, Lake Oswego, OR). Data are expressed as mean  $\pm$  s.e.m. Paired t-tests or Wilcoxon-Mann-Whitney 2-sample rank test was used to determine significance;  $P < 0.05$  was considered significant.

## Pharmacology

Apamin was purchased from Calbiochem; D-AP5, SR95531, and CGP55845 from Tocris Cookson; and SNX-482 from Peptide Institute.

## Results

To determine whether blocking SK2-containing channels in spines lacking R-type  $Ca_v2.3$   $Ca^{2+}$  channels boosts EPSPs, synaptic stimulations were delivered to the Shaffer collateral axons in the stratum radiatum in freshly prepared hippocampal slices from  $Ca_v2.3$  null mice, and EPSPs were measured from individual CA1 pyramidal neurons. After establishing a stable baseline, apamin (100 nM) was added to the bath solution. As shown in [Fig 1A and 1B](#), apamin application boosted EPSPs ( $148.2 \pm 5.4\%$ , n = 18,  $P < 0.001$ ). The increase in EPSP amplitude by apamin in mice lacking R-type  $Ca^{2+}$  channels was not different ( $p = 0.82$ ) than the boosting effect of apamin in WT mice ( $158.2 \pm 7.3\%$ , n = 13,  $p < 0.001$ ) ([Fig 1C](#)). These results indicate that  $Ca^{2+}$  influx through  $Ca_v2.3$  channels is not necessary to activate synaptic SK2-containing channels.

In contrast, SNX (300 nM) that increased EPSPs in WT mice ( $166.2.0 \pm 8.5\%$ , n = 11,  $p < 0.001$ ) did not affect EPSP amplitudes in mice lacking  $Ca_v2.3$   $Ca^{2+}$  channels ( $103.1 \pm 3.4\%$ , n = 10) ([Fig 2](#)). Similarly, SNX (300 nM) that increased EPSPs in the presence of apamin

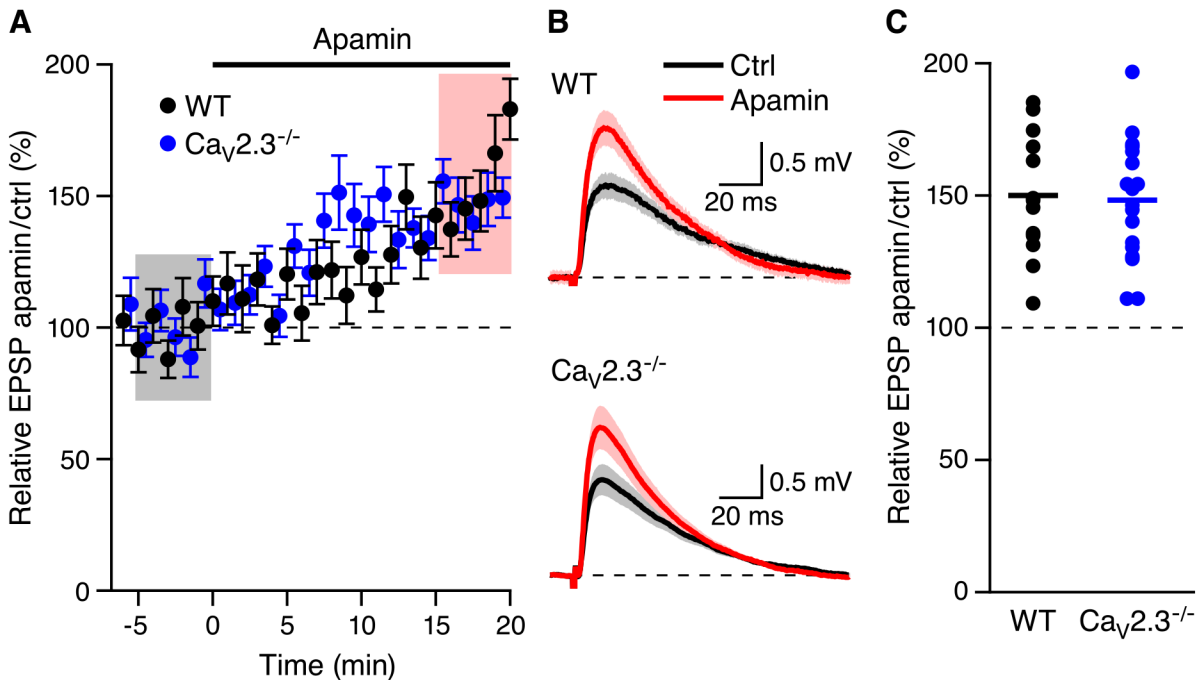


**Fig 1. Apamin boosts EPSPs in  $Ca_v2.3^{-/-}$  mice.** (A) Time course of the normalized EPSP amplitude (mean  $\pm$  s.e.m.) for baseline in control aCSF (Ctrl) and during wash-in of apamin (100 nM) as indicated above ( $n = 18$ ) in  $Ca_v2.3^{-/-}$  (blue symbols) and WT (black symbols) mice. (B) Average of 15 EPSPs taken from indicated shaded time points in aCSF (black) and 16–20 min after application of apamin (red); shaded areas are mean  $\pm$  s.e.m. (C) Scatter plot of relative EPSPs peak compared to baseline (Ctrl) from the individual slices in panel A for  $Ca_v2.3^{-/-}$  (blue symbols) and WT (black symbols). Horizontal bar reflects mean response.

doi:10.1371/journal.pone.0139332.g001

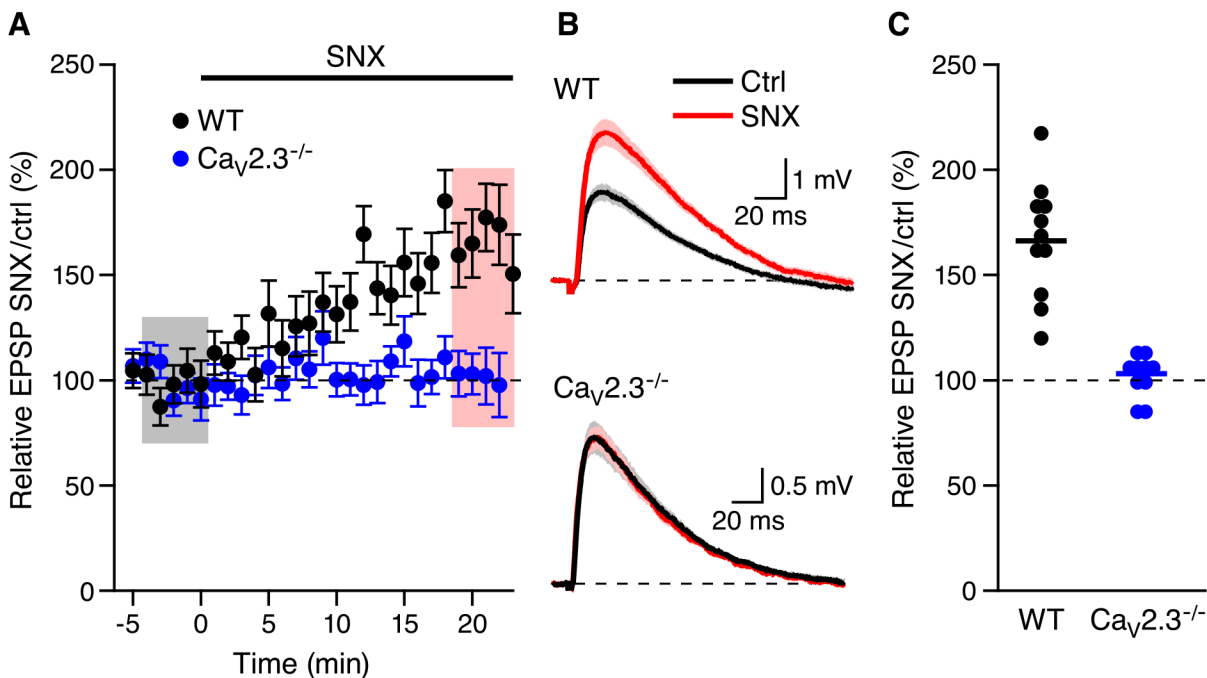


**Fig 2. Boosting of EPSPs by SNX requires  $Ca_v2.3$  R-type  $Ca^{2+}$  channels.** (A) Time course of the normalized EPSP amplitude (mean  $\pm$  s.e.m.) for baseline in control aCSF (Ctrl) and during wash-in of SNX (300 nM) as indicated above in  $Ca_v2.3^{-/-}$  (blue symbols) and WT (black symbols) mice. (B) Average of 15 EPSPs taken from indicated shaded time points in aCSF (black) and 19–23 min after application of SNX (red); shaded areas are mean  $\pm$  s.e.m. (C) Scatter plot of relative EPSPs peak compared to baseline (Ctrl) from the individual slices in panel A for  $Ca_v2.3^{-/-}$  (blue symbols) and WT (black symbols). Horizontal bar reflects mean response.

doi:10.1371/journal.pone.0139332.g002

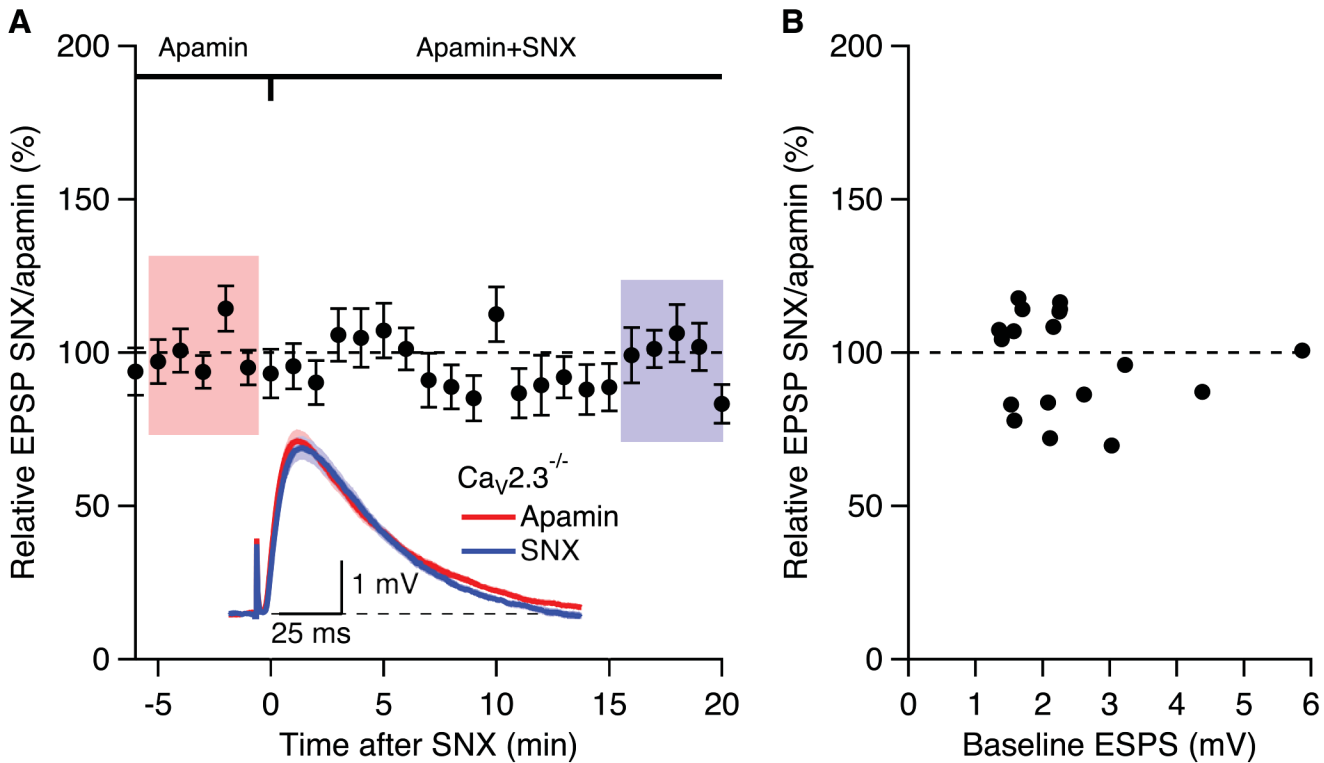


**Fig 3. Boosting of EPSPs by SNX in the presence of apamin requires  $Ca_v2.3$  R-type  $Ca^{2+}$  channels.** (A) Time course of the normalized EPSP amplitude (mean  $\pm$  s.e.m.) for baseline in apamin (100 nM) and during wash-in of SNX (300 nM) in the presence of apamin ( $n = 19$ ). Inset shows the average of 15 EPSPs taken from indicated shaded time points in apamin and 15–20 min after co-application of SNX; shaded areas are mean  $\pm$  s.e.m. (B) Plot of relative EPSPs after SNX application in the presence of apamin versus the baseline EPSP in apamin alone from all cells ( $n = 19$ ).

doi:10.1371/journal.pone.0139332.g003

in slices from WT mice ( $157.0 \pm 7.8\%$ ,  $n = 21$ ,  $p < 0.0001$ ; see Fig 1 in Wang et al., 2014 [7]) did not affect EPSP amplitudes in slices from mice lacking  $Ca_v2.3$  R-type  $Ca^{2+}$  channels pre-treated with apamin for 20–30 min ( $98.9 \pm 3.8\%$ ;  $n = 19$ ) (Fig 3A). Previously we showed that, in WT slices the apamin- and SNX-induced increase of EPSP were independent of initial EPSP size [7,11]. Fig 3B shows that the relative EPSP of SNX/apamin was independent of initial EPSP size; Fisher's  $r$  to  $z$  analysis of the EPSP increase by SNX in the presence of apamin compared to the initial EPSP size in apamin yielded no correlation. These results suggest that the SNX boosting of EPSPs in CA1 neurons require  $Ca_v2.3$  R-type  $Ca^{2+}$  channels

SNX may have off target effects as recently reported [12]. Low concentrations of  $Ni^{2+}$  (100  $\mu M$ ) have also been used to block low voltage activated T-type and R-type  $Ca^{2+}$  channels [13–16]. As shown in Fig 4  $Ni^{2+}$  (100  $\mu M$ ) increased EPSPs in WT mice ( $153.8 \pm 5.9\%$ ,  $n = 7$ ,  $P < 0.01$ ) but not in  $Ca_v2.3^{-/-}$  mice ( $92.4 \pm 4.6\%$ ,  $n = 8$ , Fig 2). The sensitivity of  $Ca_v2.3$   $Ca^{2+}$  channels to 100  $\mu M$   $Ni^{2+}$  is greatest at voltages less than -10 mV (>85% block) [17] a the voltage range that is likely not surpassed in dendritic spines during synaptic input [18]. Therefore, these results indicate that  $Ca_v2.3$  R-type  $Ca^{2+}$  channels are necessary for the boosting of EPSPs by SNX and  $Ni^{2+}$  in CA1 pyramidal neurons.

## Discussion

These results show that in the absence of  $Ca_v2.3$  R-type  $Ca^{2+}$  channels, blocking SK2-containing channels with apamin boosts synaptic responses. Consistently, in these mice, we also found that SNX or  $Ni^{2+}$  provides no additional increase to EPSPs. These findings are consistent with

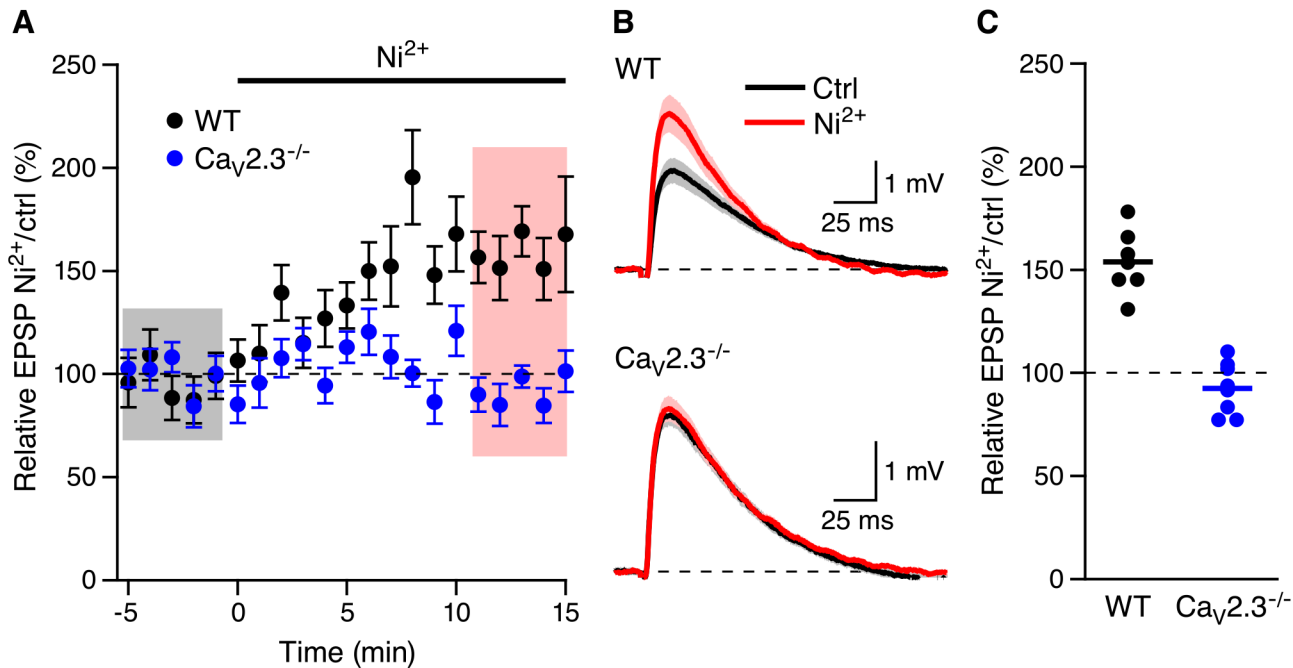


**Fig 4. Boosting of EPSPs by  $Ni^{2+}$  requires  $Ca_v2.3$  R-type  $Ca^{2+}$  channels.** (A) Time course of the normalized EPSP amplitude (mean  $\pm$  s.e.m.) for baseline in control aCSF (Ctrl) and during wash-in of 100  $\mu$ M  $Ni^{2+}$  in WT (black symbols,  $n = 7$ ) and  $Ca_v2.3^{-/-}$  mice (blue symbols, 8). (B) Average of 15 EPSPs taken from indicated shaded time points in aCSF (black) and 16–20 min after application of  $Ni^{2+}$  (red); shaded areas are mean  $\pm$  s.e.m. (C) Scatter plot of relative EPSP peak compared to baseline (Ctrl) from the individual slices in panel A for  $Ca_v2.3^{-/-}$  (blue symbols) and WT (black symbols). Horizontal bar reflects mean response.

doi:10.1371/journal.pone.0139332.g004

synaptically evoked  $Ca^{2+}$  entry through NMDARs gating the synaptic SK2-containing channels[4]. They also support previous conclusions that  $Ca^{2+}$  influx through R-type  $Ca^{2+}$  channels binds to KChIPs to increase availability of  $K_v4.2$ -containing A-type  $K^+$  channels, and blocking R-type  $Ca^{2+}$  channels with SNX or  $Ni^{2+}$  boosted synaptic potentials by decreasing availability of the repolarizing A-type  $K^+$  current[7]. Consistent with this,  $K_v4.2$  and  $Ca_v2.3$  proteins have been localized to the extrasynaptic region in CA1 spines[6,19]. This implies distinct  $Ca^{2+}$  signaling domains within the spine head, one coupling  $Ca^{2+}$  influx through NMDARs to activate SK2-containing channels and another coupling  $Ca^{2+}$  influx through R-type  $Ca^{2+}$  channels that activates  $K_v4.2$ -containing channels via KChIPs (Fig 5).

A recent report revealed that in addition to blocking R-type  $Ca^{2+}$  channels, SNX also blocks  $K_v4$ -containing channels[9]. The lack of effect of SNX and  $Ni^{2+}$  in CA1 pyramidal neurons of  $Ca_v2.3$  mice, and the previous findings using  $Ca_v2.3$  R-type  $Ca^{2+}$  channel null mice[8], support the conclusion that R-type channels are necessary for the effects SNX and  $Ni^{2+}$  in CA1 pyramidal neurons. However, the present results do not address whether SNX also blocks  $K_v4.2$ -containing  $K^+$  channels, as they may not be available to participate in synaptic responses in the absence of  $Ca^{2+}$  influx through R-type  $Ca^{2+}$  channels in  $Ca_v2.3$  null mice. Importantly, the lack of effect of  $Ni^{2+}$  and SNX in  $Ca_v2.3$  null mice supports the model that  $Ca^{2+}$  influx through R-type channels in CA1 provides the  $Ca^{2+}$  source to modulate  $K_v4.2$ -containing  $K^+$  channel availability via associated KChIPs[7]. This is in contrast to cerebellar granule and stellate cells in which T-type  $Ca^{2+}$  channels couple to A-type  $K^+$  currents and SNX had no effect A-type channel availability[10,20].

Based upon results obtained using glutamate uncaging onto single dendritic spines, a model has been proposed in which the NMDAR dependence of synaptic boosting by apamin was not

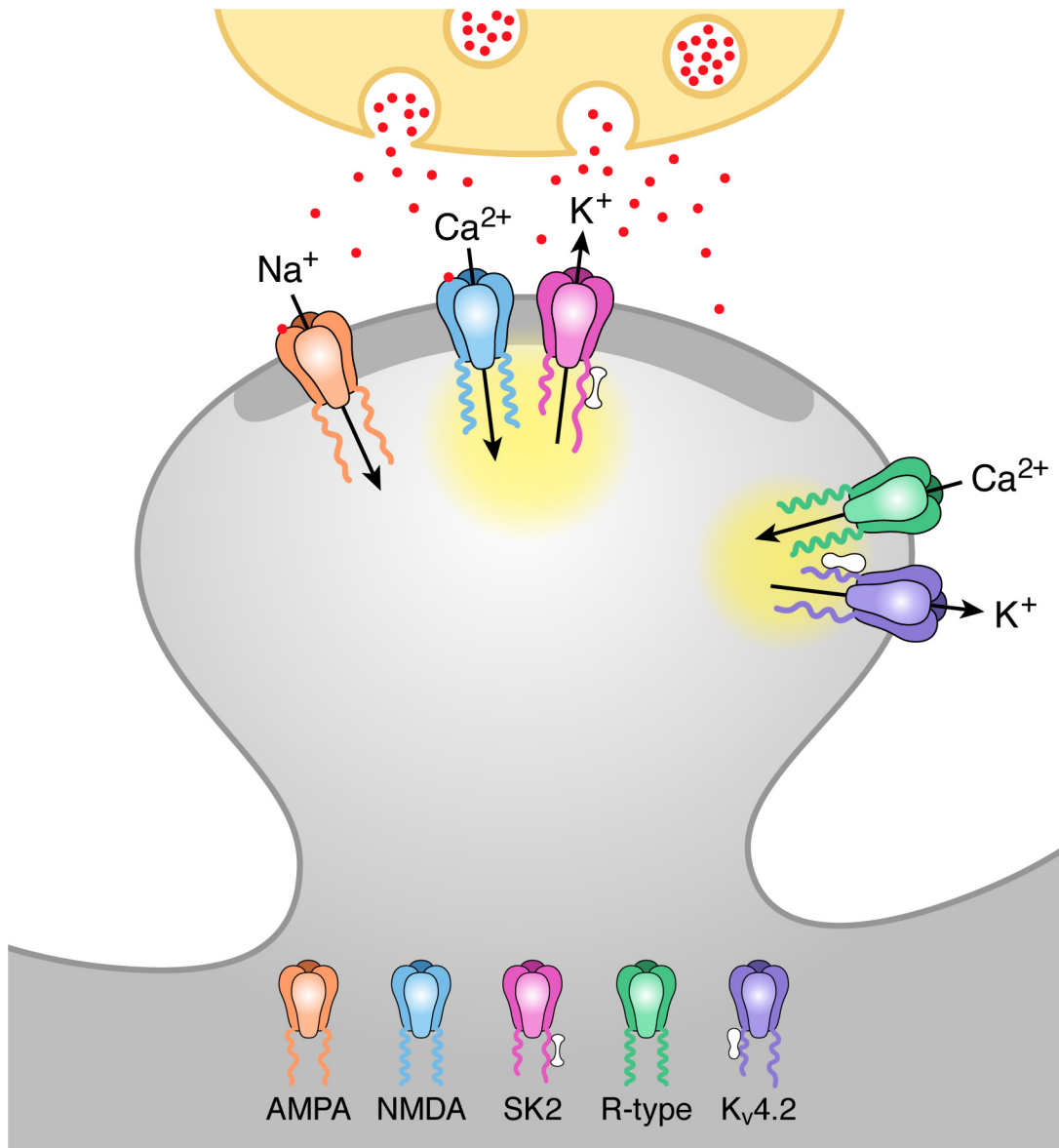


**Fig 5. Model of activation of SK2 and Kv4.2 containing channels by distinct Ca<sup>2+</sup> microdomains during synaptic stimulation.** Schaffer collateral stimulation releases glutamate (red particles) from the presynaptic terminal (ivory). Glutamate binding to AMPA and NMDA receptors in the postsynaptic density (PSD; dark grey) of the spine head depolarizes the spine membrane potential and releases voltage-dependent Mg<sup>2+</sup> block from NMDA receptors allowing for Ca<sup>2+</sup> influx during the EPSP. This Ca<sup>2+</sup> activates closely associated SK2 channels via binding to calmodulin (barbell structure) bound to C-terminus of SK2 subunits. Spine depolarization also activates R-type Ca<sup>2+</sup> channels located extrasynaptically that are close to Kv4.2-containing K<sup>+</sup> channels. Ca<sup>2+</sup> entering through R-type channels binds to KChIPs (peanut structure) associated with Kv4.2 channels shifting the voltage-dependence of availability to more negative potentials and allowing for Kv4.2 activation during an EPSP. The yellow clouds represent the microdomain for each Ca<sup>2+</sup> source.

doi:10.1371/journal.pone.0139332.g005

directly due to Ca<sup>2+</sup> influx through NMDARs activating SK2-containing channels. Rather than NMDAR activation provided a necessary component of depolarization that activated R-type Ca<sup>2+</sup> channels, and they provided the Ca<sup>2+</sup> to fuel SK2-containing channel activation[5]. The present results used synaptic stimulations and suggest alternate conclusions. It should be noted that there are several distinctions between these studies that may be very significant. First, Kv4.2 and SK2 expression change with age[21,22] and the ages of the animals employed are different, P 16–18 for the uncaging studies while we used 4–8 week old mice. Second, we

cannot be precisely sure of the location of the spines that are stimulated while the uncaging studies used spines on first oblique branches within 100 μm of the soma. Third, we do not know the nature of the stimulated spines, and the uncaging studies chose mushroom type spines. Given these differences, and while we cannot rule out the possibility that in the absence of R-type Ca<sup>2+</sup> channels, the Ca<sup>2+</sup> signaling domain architecture in the spine head is compromised, the present results are more consistent with Ca<sup>2+</sup> influx through NMDARs fueling SK2-containing channel activation, a model supported by immuno-electron microscopy that showed close anatomical localization of SK2 and NMDAR within the PSD [3].

## Acknowledgments

We thank Dr. Miller for the generous gift of Ca<sub>v</sub>2.3 null mice.

## Author Contributions

Conceived and designed the experiments: JPA JM. Performed the experiments: KW MHK WWW. Analyzed the data: JM. Wrote the paper: JPA JM.

## References

1. Nimchinsky EA, Sabatini BL, Svoboda K. Structure and function of dendritic spines. *Annu Rev Physiol*. 2002; 64: 313–353. doi: [10.1146/annurev.physiol.64.081501.160008](https://doi.org/10.1146/annurev.physiol.64.081501.160008) PMID: [11826272](https://pubmed.ncbi.nlm.nih.gov/11826272/)
2. Dumitriu D, Rodriguez A, Morrison JH. High-throughput, detailed, cell-specific neuroanatomy of dendritic spines using microinjection and confocal microscopy. *Nat Protoc*. 2011; 6: 1391–1411. doi: [10.1038/nprot.2011.389](https://doi.org/10.1038/nprot.2011.389) PMID: [21886104](https://pubmed.ncbi.nlm.nih.gov/21886104/)
3. Lin MT, Luján R, Watanabe M, Adelman JP, Maylie J. SK2 channel plasticity contributes to LTP at Schaffer collateral-CA1 synapses. *Nat Neurosci*. 2008; 11: 170–177. doi: [10.1038/nn2041](https://doi.org/10.1038/nn2041) PMID: [18204442](https://pubmed.ncbi.nlm.nih.gov/18204442/)
4. Ngo-Anh TJ, Bloodgood BL, Lin M, Sabatini BL, Maylie J, Adelman JP. SK channels and NMDA receptors form a Ca<sup>2+</sup>-mediated feedback loop in dendritic spines. *Nat Neurosci*. 2005; 8: 642–649. doi: [10.1038/nn1449](https://doi.org/10.1038/nn1449) PMID: [15852011](https://pubmed.ncbi.nlm.nih.gov/15852011/)
5. Bloodgood BL, Sabatini BL. Nonlinear regulation of unitary synaptic signals by Ca<sub>v</sub>(2.3) voltage-sensitive calcium channels located in dendritic spines. *Neuron*. 2007; 53: 249–260. doi: [10.1016/j.neuron.2006.12.017](https://doi.org/10.1016/j.neuron.2006.12.017) PMID: [17224406](https://pubmed.ncbi.nlm.nih.gov/17224406/)
6. Parajuli LK, Nakajima C, Kulik A, Matsui K, Schneider T, Shigemoto R, et al. Quantitative Regional and Ultrastructural Localization of the Cav2.3 Subunit of R-type Calcium Channel in Mouse Brain. *J Neurosci*. 2012; 32: 13555–13567. doi: [10.1523/JNEUROSCI.1142-12.2012](https://doi.org/10.1523/JNEUROSCI.1142-12.2012) PMID: [23015445](https://pubmed.ncbi.nlm.nih.gov/23015445/)
7. Wang K, Lin MT, Adelman JP, Maylie J. Distinct Ca<sup>2+</sup> sources in dendritic spines of hippocampal CA1 neurons couple to SK and KV4 channels. *Neuron*. Elsevier; 2014; 81: 379–387. doi: [10.1016/j.neuron.2013.11.004](https://doi.org/10.1016/j.neuron.2013.11.004) PMID: [24462100](https://pubmed.ncbi.nlm.nih.gov/24462100/)
8. Giessel AJ, Sabatini BL. Boosting of synaptic potentials and spine Ca transients by the peptide toxin SNX-482 requires alpha-1E-encoded voltage-gated Ca channels. *PLoS ONE*. 2011; 6: e20939. doi: [10.1371/journal.pone.0020939](https://doi.org/10.1371/journal.pone.0020939) PMID: [21695265](https://pubmed.ncbi.nlm.nih.gov/21695265/)
9. Kimm T, Bean BP. Inhibition of A-Type Potassium Current by the Peptide Toxin SNX-482. *Journal of Neuroscience*. 2014; 34: 9182–9189. doi: [10.1523/JNEUROSCI.0339-14.2014](https://doi.org/10.1523/JNEUROSCI.0339-14.2014) PMID: [25009251](https://pubmed.ncbi.nlm.nih.gov/25009251/)
10. Heath NC, Rizwan AP, Engbers JDT, Anderson D, Zamponi GW, Turner RW. The Expression Pattern of a Cav3-Kv4 Complex Differentially Regulates Spike Output in Cerebellar Granule Cells. *Journal of Neuroscience*. 2014; 34: 8800–8812. doi: [10.1523/JNEUROSCI.0981-14.2014](https://doi.org/10.1523/JNEUROSCI.0981-14.2014) PMID: [24966380](https://pubmed.ncbi.nlm.nih.gov/24966380/)
11. Lin MT, Luján R, Watanabe M, Frerking M, Maylie J, Adelman JP. Coupled activity-dependent trafficking of synaptic SK2 channels and AMPA receptors. *Journal of Neuroscience*. 2010; 30: 11726–11734. doi: [10.1523/JNEUROSCI.1411-10.2010](https://doi.org/10.1523/JNEUROSCI.1411-10.2010) PMID: [20810893](https://pubmed.ncbi.nlm.nih.gov/20810893/)
12. Bourinet E, Bourinet E, Stotz SC, Stotz SC, Spaetgens RL, Spaetgens RL, et al. Interaction of SNX482 with domains III and IV inhibits activation gating of alpha(1E) (Ca(V)2.3) calcium channels. *Biophys J*. Elsevier; 2001; 81: 79–88. doi: [10.1016/S0006-3495\(01\)75681-0](https://doi.org/10.1016/S0006-3495(01)75681-0)
13. Tsien RW, Ellinor PT, Horne WA. Molecular diversity of voltage-dependent Ca<sup>2+</sup> channels. *Trends Pharmacol Sci*. 1991; 12: 349–354. Available: <http://eutils.ncbi.nlm.nih.gov/entrez/eutils/elink.fcgi?dbfrom=pubmed&id=1659003&retmode=ref&cmd=prlinks> PMID: [1659003](https://pubmed.ncbi.nlm.nih.gov/1659003/)



14. Zhang JF, Randall AD, Ellinor PT, Horne WA, Sather WA, Tanabe T, et al. Distinctive pharmacology and kinetics of cloned neuronal  $Ca^{2+}$  channels and their possible counterparts in mammalian CNS neurons. *Neuropharmacology*. 1993; 32: 1075–1088. PMID: [8107963](#)
15. Lee JH, Gomora JC, Cribbs LL, Perez-Reyes E. Nickel block of three cloned T-type calcium channels: low concentrations selectively block  $\alpha_1H$ . *Biophys J*. 1999; 77: 3034–3042. doi: [10.1016/S0006-3495\(99\)77134-1](#) PMID: [10585925](#)
16. Sochivko D, Pereverzev A, Smyth N, Gissel C, Schneider T, Beck H. The  $Ca(V)2.3$   $Ca^{2+}$  channel subunit contributes to R-type  $Ca^{2+}$  currents in murine hippocampal and neocortical neurones. *J Physiol (Lond)*. 2002; 542: 699–710.
17. Zamponi GW, Bourinet E, Snutch TP. Nickel block of a family of neuronal calcium channels: subtype- and subunit-dependent action at multiple sites. *J Membr Biol*. 1996; 151: 77–90. PMID: [8661496](#)
18. Palmer LM, Stuart GJ. Membrane potential changes in dendritic spines during action potentials and synaptic input. *J Neurosci*. 2009; 29: 6897–6903. doi: [10.1523/JNEUROSCI.5847-08.2009](#) PMID: [19474316](#)
19. Kim J, Jung S-C, Clemens AM, Petralia RS, Hoffman DA. Regulation of dendritic excitability by activity-dependent trafficking of the A-type  $K^+$  channel subunit  $Kv4.2$  in hippocampal neurons. *Neuron*. 2007; 54: 933–947. doi: [10.1016/j.neuron.2007.05.026](#) PMID: [17582333](#)
20. Anderson D, Mehaffey WH, Iftinca M, Rehak R, Engbers JDT, Hameed S, et al. Regulation of neuronal activity by  $Ca_v3$ - $Kv4$  channel signaling complexes. *Nat Neurosci*. 2010; 13: 333–337. doi: [10.1038/nn.2493](#) PMID: [20154682](#)
21. Maletic-Savatic M, Lenn NJ, Trimmer JS. Differential spatiotemporal expression of  $K^+$  channel polypeptides in rat hippocampal neurons developing in situ and in vitro. *J Neurosci*. 1995; 15: 3840–3851. PMID: [7751950](#)
22. Ballesteros-Merino C, Lin M, Wu WW, Ferrandiz-Huertas C, Cabañero MJ, Watanabe M, et al. Developmental profile of SK2 channel expression and function in CA1 neurons. *Hippocampus*. 2012; 22: 1467–1480. doi: [10.1002/hipo.20986](#) PMID: [22072564](#)